Partition of unity for localization in implicit *a posteriori* finite element error control for linear elasticity

Carsten Carstensen[1, *, †] and Jan Thiele[2, ‡]

[1]*Department of Mathematics, Humboldt-Universität zu Berlin, Unter den Linden 6, Berlin D-10099, Germany*
[2]*BMW Group, Hufelandstraße, 8a, München D-80788, Germany*

SUMMARY

The partition of unity for localization in adaptive finite element method (FEM) for elliptic partial differential equations has been proposed in Carstensen and Funken (*SIAM J. Sci. Comput.* 2000; **21**: 1465–1484) and is applied therein to the Laplace problem. A direct adaptation to linear elasticity in this paper yields a first estimator η_L based on patch-oriented local-weighted interface problems. The global Korn inequality with a constant C_{Korn} yields reliability $\|u - u_h\| \leqslant C_{Korn}\eta_L$ for any finite element approximation u_h to the exact displacement u. In order to localize this inequality further and so to involve the global constant C_{Korn} directly in the local computations, we deduce a new error estimator μ_L. The latter estimator is based on local-weighted interface problems with rigid body motions (RBM) as a kernel and so leads to effective estimates only if RBM are included in the local FE test functions. Therefore, the excluded first-order FEM has to be enlarged by RBM, which leads to a partition of unit method (PUM) with RBM, called $P_1 + RBM$, or to second-order FEMs, called P_2 FEM. For $P_1 + RBM$ and P_2 FEM (or even higher-order schemes) one obtains the sharper reliability estimate $\|u - u_h\| \leqslant \mu_L$. Efficiency holds in the strict sense of $\mu_L \lesssim \|u - u_h\|$.

The local-weighted interface problems behind the implicit error estimators η_L and μ_L are usually not exactly solvable and are rather approximated by some FEM on a refined mesh and/or with a higher-order FEM. The computable approximations $\tilde{\eta}_L \leqslant \eta_L$ and $\tilde{\mu}_L \leqslant \mu_L$ are shown to be reliable in the sense of $\|u - u_h\| \lesssim \min\{\tilde{\eta}_L, \tilde{\mu}_L\} + osc$. The oscillations osc are known functions of the given data and higher-order terms if the data are smooth for first-order FEM.

The mathematical proofs are based on weighted Korn inequalities and inverse estimates combined with standard arguments. The numerical experiments for uniform and adapted FEM on benchmarks such as an L-shape problem, Cook's membrane, or a slit problem validate the theoretical estimates and also concern numerical bounds for C_{Korn} and the locking phenomena. Copyright © 2007 John Wiley & Sons, Ltd.

---

*Correspondence to: Carsten Carstensen, Department of Mathematics, Humboldt-Universität zu Berlin, Unter den Linden 6, Berlin D-10099, Germany.
†E-mail: cc@math.hu-berlin.de
‡E-mail: jan.thiele@bmw.de

1. INTRODUCTION

Residual-based *a posteriori* error estimators for a finite element method (FEM) with computed approximation u_h for the unknown exact displacement u are well established in computational mechanics [1–6]. A typical form of an explicit estimator reads η_R with

$$\eta_R^2 := \sum_{T \in \mathscr{T}} \eta_T^2 + \sum_{E \in \mathscr{E}} \eta_E^2$$

with local contributions: The volume contribution of one element $\eta_T^2 = h_T^2 \| \operatorname{div} \sigma_h + f \|_{L^2(T)}$ is the residual $\operatorname{div} \sigma(u_h) + f$ on each element $T \in \mathscr{T}$, $\mathscr{T}$ is the triangulation (the set of element domains) of the domain Ω, taken in L^2-norm over the triangle and weighted with the local mesh size $h_T := \operatorname{diam}(T)$; the edge contribution $\eta_E^2 := h_E \| J_j \|_{2,E}$ is the jump of the discrete stress field σ_h with its jump J_h of its normal component taken in its L^2-norm over the edge and weighted with the local mesh size $h_E := \operatorname{diam}(E)$.

The estimator η_R is known to be efficient and reliable in the sense that there exist constants $C_{R,\text{eff}}$ and $C_{R,\text{rel}}$ and higher-order terms such that there holds

$$C_{R,\text{eff}} \eta_R - \text{h.o.t.} \leqslant \| u - u_h \|_{1,2} \leqslant C_{R,\text{rel}} \eta_R + \text{h.o.t.}$$

The constants $C_{R,\text{eff}}$ and $C_{R,\text{rel}}$ do not depend on the mesh sizes h_T or h_E but in a mild form on the minimal angle or the largest aspect ratio of the element domains in a (shape) regular triangulation. In elasticity, the constants may well depend on the material parameter. Note also that $\| u - u_h \|_{1,2}$ is the error $u - u_h$ in its semi-norm which is equivalent to the energy norm; but again, the equivalence constants depend on the material parameter.

Moreover, it is observed in [7] for the Poisson problem, that the strict estimation of $C_{R,\text{eff}}$ and $C_{R,\text{rel}}$ is (almost) useless as a termination criterion: the overestimation is up to a factor 10 and much higher in practical examples. For sharp error control, one requires implicit error estimators such as the equilibration error estimator η_{EQ} [8] or the patch-residual error estimator η_{L} [9–11].

A direct adaptation to linear elasticity in this paper yields a first estimator η_{L} which is based on patch-oriented local-weighted interface problems. The global Korn inequality with a constant C_{Korn} yields reliability $\| u - u_h \| \leqslant C_{\text{Korn}} \eta_{\text{L}}$ for any finite element approximation u_h to the exact displacement u. In order to localize this inequality further and so to involve the global constant C_{Korn} directly in the local computations, one deduces a related but new error estimator μ_{L}. The latter estimator is based on local-weighted interface problems with rigid body motions (RBM) as a kernel and so leads to effective estimates only if RBM are included in the local FE test functions. Therefore, the excluded first-order FEM have to be enlarged by RBM, which leads to a partition of unit method (PUM) with RBM, called $P_1 + \text{RBM}$, or to second-order FEMs, called P_2 FEM. For $P_1 + \text{RBM}$ and P_2 FEM (or even higher-order schemes) one obtains the sharper reliability estimate $\| u - u_h \| \leqslant \mu_{\text{L}}$. Efficiency holds in the strict sense of $\mu_{\text{L}} \lesssim \| u - u_h \|$. In the following, $a \lesssim b$ abbreviates $a \leqslant C b$ with a multiplicative generic constant C.

The local-weighted interface problems behind η_{L} and μ_{L} are usually not exactly solvable but are rather approximated by some FEM on a refined mesh and/or with a higher-order FEM. The computable approximations $\tilde{\eta}_{\text{L}} \leqslant \eta_{\text{L}}$ and $\tilde{\mu}_{\text{L}} \leqslant \mu_{\text{L}}$ are shown to be reliable in the sense of $\| u - u_h \| \lesssim \min\{\tilde{\eta}_{\text{L}}, \tilde{\mu}_{\text{L}}\} + \text{osc}$. The oscillations osc are known functions of the given data and higher-order terms if the given data are smooth.

The mathematical proofs are based on weighted Korn inequalities and inverse estimates plus standard arguments. Numerical bounds for C_{Korn} and locking phenomena are provided as well.

The remainder of this paper is organized as follows: necessary notation and assumptions on the continuous and discrete model are summarized in Section 2. The localized error estimator η_{L} and its reliability and efficiency are established in Section 3. The constant in the local Korn's inequalities are involved in μ_{L} of Section 4 where the reliability and efficiency of μ_{L} are proved and numerical approximations of C_{GKorn} are studied. The numerical realization of the implicit *a posteriori* error estimators η_{L} and μ_{L} through their finite element approximations $\tilde{\eta}_{\text{L}}$ and $\tilde{\mu}_{\text{L}}$ is discussed in Section 5. The numerical experiments of Section 6 for uniform and adapted FEM on benchmarks such as an L-shape problem, Cook's membrane, or a slit problem validate the theoretical estimates. A brief discussion of some main results in Section 7 concludes the paper.

2. PRELIMINARIES

This section introduces the necessary notation and assumptions and presents the well-established facts about the mathematical model and its finite element discretization.

2.1. Mathematical model—Lamé–Navier equations

The elastic body $\Omega \subset \mathbb{R}^2$ is viewed as a planar-bounded Lipschitz domain with polygonal boundary $\partial\Omega = \Gamma_{\text{D}} \cup \Gamma_{\text{N}}$. It is loaded by applied volume forces $f \in L^2(\Omega; \mathbb{R}^2)$ and surface traction $g \in L^2(\Gamma_{\text{N}}; \mathbb{R}^2)$ on some (relatively open) part Γ_{N} of the boundary $\partial\Omega$ with exterior unit normal v. The elastic body is supported on the remaining closed part $\Gamma_{\text{D}} := \partial\Omega \setminus \Gamma_{\text{N}}$ where the displacement field is prescribed by the Dirichlet part $u_{\text{D}} \in H^1(\Omega; \mathbb{R}^2)$. It is important for Korn's inequality and the unique existence of weak solutions below that Γ_{D} is closed and has a positive length. The remaining case of a pure Neumann problem with $\Gamma_{\text{N}} = \partial\Omega$ and $\Gamma_{\text{D}} = \emptyset$ requires a slightly different functional analytical setting and is hence excluded here for the ease of this presentation.

A linear elastic material behaviour is modelled with the two positive Lamé parameters λ and μ which define the fourth-order isotropic material tensor $\mathbb{C}$. That is, the stress tensor σ is a linear function of the linear Green strain $\varepsilon(u) := (Du + (Du)^{\text{T}})/2$, the symmetric part of the functional matrix $Du = (u_{j,k})_{j,k=1,2}$ of all first-order partial derivatives $u_{j,k} := \partial u_j/\partial x_k$ of the (unknown) displacement field u,

$$\sigma(u) := \mathbb{C}\varepsilon(u) := \lambda \operatorname{tr}(\varepsilon(u))I + 2\mu\varepsilon(u)$$

For each material point $x \in \Omega$, $\sigma(x)$, and $\varepsilon(u)(x)$ are symmetric 2×2 matrices with the trace and a row-wise divergence, e.g. the scalar $\operatorname{tr}(\varepsilon(u)) = \operatorname{div} u = u_{1,1} + u_{2,2}$ and the vector $\operatorname{div} \sigma = (\sigma_{j,1} + \sigma_{j,2})_{j=1,2}$.

In the aforementioned notation, the *strong form* of boundary-value problem with the Lamé–Navier equations in linear elasticity reads: *seek* $u \in H^1(\Omega; \mathbb{R}^2)$ *with*

$$-\operatorname{div} \sigma(u) = f \quad \text{in } \Omega \tag{1}$$

$$\sigma(u)v = g \quad \text{on } \Gamma_{\text{N}} \tag{2}$$

$$u = u_{\text{D}} \quad \text{on } \Gamma_{\text{D}} \tag{3}$$

2.2. Weak formulation

The Sobolev space $H^1(\Omega; \mathbb{R}^2) := \{v \in L^2(\Omega; \mathbb{R}^2) : Dv \in L^2(\Omega; \mathbb{R}^{2 \times 2})\}$ consists of L^2-functions (i.e. Lebesgue measurable functions with integrables squares) with a square-integrable weak derivative Dv. Define the restriction of $H^1(\Omega; \mathbb{R}^2)$ with homogenous Dirichlet boundary values as

$$V := H^1_D(\Omega; \mathbb{R}^2) := \{v \in H^1(\Omega; \mathbb{R}^2) : v = 0 \text{ on } \Gamma_D\}$$

The weak form consists of the bilinear form $a(u, v)$ and the linear functional $b(v)$, defined by

$$a(u, v) := \int_\Omega \sigma(u) : \varepsilon(v) \, dx = \int_\Omega \mathbb{C}\varepsilon(u) : \varepsilon(v) \, dx \tag{4}$$

$$b(v) := \int_\Omega f \cdot v \, dx + \int_{\Gamma_N} g \cdot v \, ds \tag{5}$$

for all $u, v \in H^1(\Omega; \mathbb{R}^d)$. Then, given the data of Section 2.1, the weak formulation of the *Navier–Lamé equations* reads: *seek $u \in H^1(\Omega; \mathbb{R}^d)$ such that $u = u_D$ on Γ_D and that*

$$a(u, v) = b(v) \quad \text{for all } v \in V \tag{6}$$

According to the positive definiteness of the material tensor $\mathbb{C}$ and Korn's inequality, namely

$$\|Dv\|_{L^2(\Omega)} \leqslant C_{\text{Korn}} \|\varepsilon(v)\|_{L^2(\Omega)} \quad \text{for all } v \in V \tag{7}$$

$$\|Dv\|_{L^2(\Omega)} \leqslant C_{\text{Kornelast}} \|\mathbb{C}^{1/2}\varepsilon(v)\|_{L^2(\Omega)} \quad \text{for all } v \in V \tag{8}$$

the bilinear form a is a scalar product on V (here we require that Γ_D has a positive length). The unique existence of a weak solution u is then a consequence of the Riesz representation theorem in the Hilbert space (V, a). More remarks on Korn's constants and even numerical approximations will be given in Sections 6.1–6.3.

2.3. Regular triangulations

Each of the studied FEM is based on a shape-regular triangulation $\mathcal{T}$ of the domain Ω in closed triangles which is specified in the following. The set $\mathcal{T}$ consists of closed triangles with positive area such that their union $\cup \mathcal{T}$ covers the domain and its boundary

$$\cup \mathcal{T} = \overline{\Omega} = \Omega \cup \partial\Omega$$

The intersection $T \cap K$ of each pair of distinct triangles T and K in $\mathcal{T}$ satisfies one of the three conditions: $T \cap K$ is either empty, a common edge, or a common vertex also called node of the two

$$T \cap K \in \{\emptyset\} \cup \mathcal{E} \cup \mathcal{N} \cup \mathcal{T} \quad \text{for all } T, K \in \mathcal{T}$$

Here and in the following, $\mathcal{E}$ is the set of all edges (of some triangle) in $\mathcal{T}$ and $\mathcal{N}$ is the set of all nodes (or vertices of some triangle) in $\mathcal{T}$. A shape-regular triangulation is a triangulation in the aforementioned sense in which the triangles have an interior angle $\gtrsim 1$; i.e. the interior angles are bounded below away from zero uniformly (independent of the mesh sizes). All the constants below

may and will depend on the minimal angle in $\mathcal{T}$ without further mentioning this fact. [In other words, $\mathcal{T}$ has no hanging nodes and is locally quasiuniform.] Related notations are summarized below. For each element domain $T \in \mathcal{T}$ of diameter $h_T := \text{diam}(T)$ and area $|T| > 0$, $\mathcal{E}(T) \subset \mathcal{E}$ denotes the set of the three edges, $\mathcal{N}(T) \subset \mathcal{N}$ denotes the set of the three vertices or nodes. Each edge E with $E \subset \partial\Omega$ satisfies either $E \subset \Gamma_D$ or $E \subset \overline{\Gamma_N}$ and this is denoted by $E \in \mathcal{E}_D$ and $E \in \mathcal{E}_N$, respectively. All the remaining edges satisfy $E \not\subset \partial\Omega$ written $E \in \mathcal{E}_\Omega$. This defines a partition

$$\mathcal{E} = \mathcal{E}_\Omega \cup \mathcal{E}_D \cup \mathcal{E}_N$$

Given any edge $E \in \mathcal{E}$ of length $h_E := \text{diam}(E)$ there is one fixed unit normal ν_E and one unit tangential vector τ_E; $\nu = \nu_E$ for an edge $E \in \mathcal{E}_D \cup \mathcal{E}_N$ on the boundary.

For any edge $E \in \mathcal{E}$ and any element $T \in \mathcal{T}$, its midpoint (centre of inertia) is denoted as $\text{mid}(E)$ and $\text{mid}(T)$, respectively.

The hat function φ_z of some node $z \in \mathcal{N}$ is defined by the values $\varphi_z(x)$ for a node $x \in \mathcal{N}$, namely $\varphi_z(z) = 1$ and $\varphi_z(x) = 0$ for $x \in \mathcal{N} \setminus \{z\}$, followed by a linear interpolation on each triangle ($\varphi_z \in P_1(\mathcal{T})$ in the notation of the following subsection). Then, the patch of a node is the open set

$$\omega_z := \{x \in \Omega : 0 \neq \varphi(x)\}$$

which is the interior of the set $\mathcal{T}(z)$ of neighbouring elements

$$\overline{\omega_z} = \cup \mathcal{T}(z) \quad \text{where } \mathcal{T}(z) := \{T \in \mathcal{T} : z \in T\}$$

The set of free nodes $\mathcal{K} := \mathcal{N} \setminus \Gamma_D$ consists of all vertices which have a positive distance to the Dirichlet boundary Γ_D. The remaining nodes on the Dirichlet boundary read $\mathcal{N}_D := \mathcal{N} \cap \mathcal{K}$. The notation is restricted to $d = 2$ dimensions for the ease of this discussion but allows a well-established modification to $d = 3$. Although details are not always displayed, the main results of this paper hold for $d \geqslant 2$.

2.4. Three finite element methods: P_1, P_1 + RBM, P_2

The FEM is essentially described by the finite element space (FES) V_h of the test function space. The geometric boundary conditions on Γ_D are homogeneous in all three cases of $V_h \subset V$ and prescribed by u_D for each node along Γ_D (see below).

For any subset ω (patch, triangle, or edge), let $P_k(\omega)$ denote the vector space of all algebraic polynomials viewed as real-valued functions on ω of total degree at most $k = 0, 1, 2$. Then

$$P_k(\mathcal{T}) := \{v_h \in L^\infty(\Omega) : \forall T \in \mathcal{T}, \ v_h|_T \in P_k(T)\}$$

denotes the piecewise polynomials of degree at most k where piecewise is with respect to the shape-regular triangulation $\mathcal{T}$; in general, the functions in $P_k(\mathcal{T})$ are discontinuous. The globally continuous functions in $P_1(\mathcal{T})$ and $P_2(\mathcal{T})$ form the P_1 and P_2 FES

$$P_k\text{FES}(\mathcal{T})^d := (P_k(\mathcal{T}) \cap C(\overline{\Omega}))^d \quad \text{and} \quad P_{k,D}\text{FES}(\mathcal{T})^d := P_k(\mathcal{T})^d \cap V \quad \text{for } k = 1, 2$$

Observe that $(\phi_z : z \in \mathcal{N})$ is the nodal basis of $P_1\text{FES}(\mathcal{T})$ and $(\phi_z : z \in \mathcal{K})$ is the nodal basis of $P_{1,D}\text{FES}(\mathcal{T})$.

To define the partition of unity method, namely the intermediate P_1 + RBM FES, let

$$\text{RBM} := \{v \in P_1(\mathbb{R}^d; \mathbb{R}^d) : \varepsilon(v) \equiv 0\} \tag{9}$$

denote the RBMs. Their product with hat functions, namely $\{\varphi_z \, v : v \in \mathrm{RBM}\}$, is added to $P_{1,\mathrm{D}}\mathrm{FES}(\mathscr{T})$. We define a new method *via* replacing $H^1(\Omega; \mathbb{R}^d)$ by

$$V_h := P_{1,\mathrm{D}} \times \mathrm{RBM}(\mathscr{T}) := \mathrm{span}\{\varphi_z \, v : v \in \mathrm{RBM}, z \in \mathscr{K}\} \tag{10}$$

Given $u_{\mathrm{D},h}$ as a piecewise linear (for P_1 and $P_1+\mathrm{RBM}$) or piecewise quadratic (for P_2) interpolation of u_{D} along Γ_{D} extended by/to a function on Ω (by a P_1, $P_1 + \mathrm{RBM}$ or P_2 interpolation), the discrete problem reads: seek u_h in $u_{\mathrm{D},h} + V_h$ such that

$$a(u_h, v_h) = b(v_h) \quad \text{for all } v_h \in V_h \tag{11}$$

Recall that $V_h := P_k(\mathscr{T})^d \cap V$ for $k = 1, 2$ and $V_h := (P_{1,\mathrm{D}} \times \mathrm{RBM}(T))^d \cap V$ for the three FEM under consideration.

2.5. Error and residual

For a discrete FE solution u_h and the discrete stress $\sigma_h := \sigma(u_h)$ we define the volume residual $R(u_h)$ for each triangle T and the edge residual $J(u_h)$ for each edge E by

$$R(u_h) := f + \mathrm{div}_{\mathscr{T}} \sigma(u_h) \quad \text{on } T \in \mathscr{T} \tag{12}$$

$$J(u_h)|_E := [\sigma_h]\nu_E = \begin{cases} 0 & \text{for } E \in \mathscr{E}_{\mathrm{D}} := \mathscr{E} \cap \Gamma_{\mathrm{D}} \\ \sigma_h \nu_E - g & \text{for } E \in \mathscr{E}_{\mathrm{N}} := \mathscr{E} \cap \Gamma_{\mathrm{N}} \\ (\sigma_h^+|_{T_+} - \sigma_h^-|_{T_-})\nu_E & \text{for } E \in \mathscr{E}_\Omega := \mathscr{E} \setminus (\mathscr{E}_{\mathrm{N}} \cup \mathscr{E}_{\mathrm{D}}) \end{cases} \tag{13}$$

Here and throughout $\mathrm{div}_{\mathscr{T}}$ is the elementwise-defined divergence and $E = \partial T_+ \cap \partial T_- \in \mathscr{E}_\Omega$ and two distinct $T_\pm \in \mathscr{T}$. An elementwise integration by parts proves that the functional

$$\mathrm{Res} := b - a(u_h, \cdot) \in V^*$$

equals, for any argument $v \in V$,

$$\mathrm{Res}(v) = (R(u_h), v)_{L^2(\Omega)} - \sum_{E \in \mathscr{E}} \int_E J(u_h) v \, \mathrm{d}s$$

The error $e := u - u_h$ is defined for the exact solution $u \in H^1(\Omega; \mathbb{R}^d)$ of (8) and some discrete solution u_h from Section 2.4 computed by one of the P_1, $P_1 + \mathrm{RBM}$, P_2 FEMs. The energy norm $\||\cdot\||$ of a displacement $w \in H^1(\Omega; \mathbb{R}^d)$ is defined by

$$\||w\||^2 := \|\mathbb{C}^{1/2}\varepsilon(w)\|^2_{L^2(\Omega)} := \int_\Omega \varepsilon(w) : \mathbb{C}\varepsilon(w) \, \mathrm{d}x = a(w, w)$$

Since this paper does not focus on non-homogeneous Dirichlet conditions, these are described in an abstract form by η_{D} only. Recall that displacements in $V_h \subseteq V$ vanish along Γ_{D} while $(u - u_h)|\Gamma_{\mathrm{D}} = u_{\mathrm{D}} - u_{\mathrm{D},h}$ does not. Hence

$$\eta_{\mathrm{D}} := \inf_{\substack{w \in H^1(\Omega; \mathbb{R}^d) \\ w|_{\Gamma_{\mathrm{D}}} = u_{\mathrm{D}} - u_{\mathrm{D},h}}} \||w\||$$

is non-zero (but of higher order when u_D is smooth). Then set

$$\||\mathrm{Res}\||_* := \sup_{v \in V \setminus \{0\}} \mathrm{Res}(v)/\||v\||$$

$$\||\mathrm{Res}\||_{-1} := \sup_{v \in V \setminus \{0\}} \mathrm{Res}(v)/\|Dv\|_{L^2(\Omega)}$$

Note that (7) implies

$$\||\mathrm{Res}\||_* \leqslant C_{\mathrm{Kornelast}} \||\mathrm{Res}\||_{-1} \tag{14}$$

Theorem 2.1
The following bounds hold $\eta_D \leqslant \||e\||$, $\||\mathrm{Res}\||_* \leqslant \||e\||$, and $\||e\||^2 \leqslant \eta_D^2 + \||\mathrm{Res}\||_*^2$.

Proof
This is essentially well known, we give the proof for completeness: let $v \in V$ be minimizing $a(e+v, e+v)$ and $w := e+v$. Then $\||e+v\|| = \eta_D$ and $a(e+v, \cdot) = 0$ on V and

$$\||e\||^2 = \||e+v\||^2 + \||v\||^2 = \eta_D^2 - a(e, v)$$

$$\leqslant \eta_D^2 + \||\mathrm{Res}\||_* \||v\||$$

$$= \eta_D^2 + \||\mathrm{Res}\||_* (\||e\||^2 - \eta_D^2)^{1/2}$$

This proves $\eta_D^2 \leqslant \||e\||^2 \leqslant \eta_D^2 + \||\mathrm{Res}\||_*^2$. The remaining assertion $\||\mathrm{Res}\||_* \leqslant \||e\||$ follows immediately from the definition of $\||\mathrm{Res}\||_*$. $\qquad\square$

3. LOCALIZED ERROR ESTIMATOR η_L

This section is devoted to a first localization approach. It is straightforward in the sense that it is an immediate generalization of the ideas from [9] and treats the residual of the elastic problem as if it was a residual of a vector Laplace problem.

3.1. Definition of η_L

For the FE solution u_h, define the functional $\mathrm{Res}_z(v)$ for v in $V := H_D^1(\Omega; \mathbb{R}^d)$ by

$$\mathrm{Res}_z(v) := \int_{\omega_z} \varphi_z R(u_h) \cdot v \, \mathrm{d}x - \int_{\mathscr{E}_\Omega \cap \omega_z} \varphi_z J(u_h) \cdot v \, \mathrm{d}s$$

For each node z in $\mathscr{N}$ define η_z as

$$\eta_z := \sup_{\varphi_z v \not\equiv 0, v \in V} \mathrm{Res}_z(v)/\|\varphi_z^{1/2} Dv\|_{L^2(\omega_z)}$$

and as a global error estimator define η_L by $\eta_L^2 := \sum_{z \in \mathscr{N}} \eta_z^2$.

3.2. Reliability of η_L

The error estimator η_L is reliable.

Theorem 3.1 (Reliability of η_L)
Assume that u is the solution of the model problem (6) and that u_h solves the discrete problem (11) for P_1, $P_1 + \mathrm{RBM}$, or P_2 FEM. Then

$$\|\mathrm{Res}\|_{-1} \leqslant \eta_L \quad \text{and} \quad \|\mathrm{Res}\|_* \leqslant C_{\mathrm{Kornelast}}\eta_L \tag{15}$$

The constant $C_{\mathrm{Kornelast}}$ is defined by (8).

Proof
Let $v \in V$. An integration by parts, the Galerkin orthogonality, and the partition of unity $\sum_{\mathcal{N}} \varphi_z = 1$ lead to

$$\mathrm{Res}(v) = \int_\Omega (f + \mathrm{div}_{\mathcal{T}} \sigma_h) \cdot v \, dx - \sum_{E \in \mathscr{E}_\Omega} \int_E [\sigma_h] v_E \cdot v \, ds$$

$$= \sum_{z \in \mathcal{N}} \left(\int_\Omega \varphi_z (f + \mathrm{div}_{\mathcal{T}} \sigma_h) \cdot v \, dx - \int_{\mathscr{E}_\Omega} \varphi_z [\sigma_h] v_E \cdot v \, ds \right)$$

$$= \sum_{z \in \mathcal{N}} \mathrm{Res}_z(v) \leqslant \sum_{z \in \mathcal{N}} \eta_z \|\varphi_z^{1/2} Dv\|_{L^2(\omega_z)}$$

$$\leqslant \eta_L \left(\sum_{z \in \mathcal{N}} \|\varphi^{1/2} Dv\|_{L^2(\omega_z)} \right)^{1/2} = \eta_L \|Dv\|_{L^2(\Omega)}$$

This proves the first inequality of (15); the second follows from (8). $\qquad\square$

3.3. Efficiency of η_L

The proof of efficiency of η_L requires a weighted Poincaré–Friedrichs inequality. Define $\| \cdot \|_z := a_z(\cdot, \cdot)^{1/2}$ and distinguish two cases for V_z, namely

$$V_z := \begin{cases} \{v \in H^1_{\mathrm{loc}}(\omega_z) : \|\varphi_z^{1/2} Dv\|_{L^2(\omega_z)} < \infty \text{ and } v|_{\Gamma_D} = 0\} & \text{if } z \in \Gamma_D \\ \left\{v \in H^1_{\mathrm{loc}}(\omega_z) : \|\varphi_z^{1/2} Dv\|_{L^2(\omega_z)} < \infty \text{ and } \int_{\omega_z} v \, dx = 0\right\} & \text{if } z \in \mathscr{H} \end{cases}$$

For the following tool and throughout this subsection let $d = 2$ and let $\mathcal{T}$ consist of triangles.

Theorem 3.2 (Weighted Poincaré–Friedrichs inequality)
For $v \in V_z$

$$\|v\|_{L^2(\omega_z)} \leqslant C_{\mathrm{PF}} \, \mathrm{diam}(\omega_z) \|\varphi_z^{1/2} Dv\|_{L^2(\omega_z)}$$

The constant C_{PF} depends on the shape [and the boundary conditions] of the patch, but not on its size.

Proof
See [9, 10].   □

Theorem 3.3 (*Efficiency of η_L*)
Assume u is the solution of the model problem (6) and u_h is the solution of the discrete problem (11). Then, for every node $z \in \mathcal{N}$,

$$A_z := \sup_{v \in V_z} \|\mathbb{C}^{1/2}\varepsilon(\varphi_z v)\|_{L^2(\omega_z)} / \|\varphi_z^{1/2} Dv\|_{L^2(\omega_z)} < \infty \tag{16}$$

and

$$\eta_z \leqslant A_z \|\mathbb{C}^{1/2}\varepsilon(u - u_h)\|_{L^2(\omega_z)} \tag{17}$$

With $C_A := \max_{z \in \mathcal{N}} A_z$ there holds efficiency of η_L in the sense of

$$\eta_L \leqslant \sqrt{3} C_A \|\mathbb{C}^{1/2}\varepsilon(u - u_h)\|_{L^2(\Omega)} \tag{18}$$

Proof
Given any $v \in V_z$, the product rule leads to

$$\|\mathbb{C}^{1/2}\varepsilon(\varphi_z v)\|^2_{L^2(\Omega)} = \lambda \|\operatorname{div}(\varphi_z v)\|^2_{L^2(\Omega)} + 2\mu\|\varepsilon(\varphi_z v)\|^2_{L^2(\Omega)}$$

$$\leqslant \lambda \|\varphi_z(\operatorname{div} v) + v \cdot D\varphi_z\|^2_{L^2(\Omega)} + 2\mu\|\varphi_z(Dv) + v \otimes D\varphi_z\|^2_{L^2(\Omega)}$$

This and Theorem 3.2 prove

$$\|\mathbb{C}^{1/2}\varepsilon(\varphi_z v)\|_{L^2(\Omega)} \leqslant \lambda^{1/2}\sqrt{2}\|\varphi_z Dv\|_{L^2(\Omega)} + \lambda^{1/2}\|D\varphi_z\|_{L^\infty(\Omega)}\|v\|_{L^2(\omega_z)} + (2\mu)^{1/2}\|\varphi_z Dv\|_{L^2(\Omega)}$$

$$+ (2\mu)^{1/2}\|\varphi_z\|_{L^\infty(\Omega)}\|v\|_{L^2(\omega_z)}$$

$$\leqslant ((2\lambda)^{1/2} + (2\mu)^{1/2})(1 + C_{\text{PF}}\operatorname{diam}(\omega_z)\|D\varphi_z\|_{L^\infty(\Omega)})\|\varphi_z^{1/2}Dv\|_{L^2(\omega_z)}$$

Since $|D\varphi_z|\operatorname{diam}(\omega_z) < \infty$ is bounded from above independently of the mesh size, this proves $A_z < \infty$.

An integration by parts, a Cauchy inequality, and (16) yield for any $v \in V_z$

$$\operatorname{Res}_z(v) = \int_{\omega_z} \varphi_z(f + \operatorname{div}_{\mathcal{T}}\sigma_h) \cdot v \, dx - \int_{\cup \mathcal{E} \cap \omega_z} \varphi_z[\sigma_h]v_E \cdot v \, ds$$

$$= \int_{\omega_z} \mathbb{C}\varepsilon(u - u_h) : \varepsilon(\varphi_z v) \, dx$$

$$\leqslant \|\mathbb{C}^{1/2}\varepsilon(u - u_h)\|_{L^2(\omega_z)}\|\mathbb{C}^{1/2}\varepsilon(\varphi_z v)\|_{L^2(\omega_z)}$$

$$\leqslant \|\mathbb{C}^{1/2}\varepsilon(u - u_h)\|_{L^2(\omega_z)} A_z \|\varphi_z^{1/2}Dv\|_{L^2(\omega_z)}$$

This proves (17). Equation (18) follows from

$$\eta_L^2 = \sum_{z \in \mathcal{N}} \eta_z^2 \leqslant \sum_{z \in \mathcal{N}} C_A^2\|\mathbb{C}^{1/2}\varepsilon(u - u_h)\|^2_{L^2(\omega_z)} \leqslant 3C_A^2\|\mathbb{C}^{1/2}\varepsilon(u - u_h)\|^2_{L^2(\Omega)} \qquad □$$

3.4. Remarks on η_L

The usability of η_L is limited, because $C_{\text{Kornelast}}$ is an unknown global constant which enters the estimate of $\|\text{Res}\|_*$ and so of $\|e\|$. This motivates another estimator μ_L in Section 4. There, the solvability of the local problems is an important issue. The arguments for η_L can be adopted from [9, 10]. It turns out that the definition of V_z implies for each node $z \in \mathcal{N}$ that there exists a unique solution $v_z \in V_z$ with

$$\int_\Omega \varphi_z D v_z \cdot D w \, \mathrm{d}x = \text{Res}_z(w) \quad \text{for all } w \in V_z \tag{19}$$

Moreover

$$\eta_z = \|\varphi_z^{1/2} D v_z\|_{L^2(\omega_z)} \tag{20}$$

4. LOCALIZED ERROR ESTIMATOR μ_L

4.1. Definition of μ_L

For each node z in $\mathcal{N}$ define μ_z by

$$\mu_z := \sup_{\varphi_z^{1/2} \mathbb{C}^{1/2} \varepsilon(v) \not\equiv 0, \, v \in V} \text{Res}_z(v) / \|\varphi_z^{1/2} \mathbb{C}^{1/2} \varepsilon(v)\|_{L^2(\omega_z)}$$

As a global error estimator define

$$\mu_L := \left(\sum_{z \in \mathcal{N}} \mu_z^2 \right)^{1/2}$$

At this stage, $\mu_z = \infty$ and $\mu_L = \infty$ are possible and below we will exclude the P_1 FEM.

4.2. Reliability of μ_L

Assume u to be the solution of the model problem and u_h a numerical approximation of u obtained by an appropriate FEM.

Theorem 4.1
We have the following bound on μ_L

$$\|\mathbb{C}^{1/2} \varepsilon(u - u_h)\|_{L^2(\Omega)} \leqslant \mu_L \tag{21}$$

Proof
This is obtained along the arguments of the previous proofs indicated in the following:

$$\|\mathbb{C}^{1/2} \varepsilon(u - u_h)\|_{L^2(\Omega)}^2 = \int_\Omega \varepsilon(u - u_h) : \mathbb{C} \varepsilon(u - u_h) \, \mathrm{d}x$$

$$\leqslant \sum_{z \in \mathcal{N}} \mu_z \|\varphi_z^{1/2} \mathbb{C}^{1/2} \varepsilon(u - u_h)\|_{L^2(\Omega)}$$

$$\leqslant \mu_L \|\mathbb{C}^{1/2} \varepsilon(u - u_h)\|_{L^2(\Omega)} \qquad \square$$

4.3. Weighted Korn's inequality

The proof of efficiency of μ_{L} requires a weighted Korn's inequality. This section aims to prove that there exists a constant C_{WKorn}, such that there holds

$$\|\varphi_z^{1/2} Dw\|_{L^2(\omega_z)} \leqslant C_{\mathrm{WKorn}} \|\varphi_z^{1/2} \varepsilon(w)\|_{L^2(\omega_z)} \quad \text{for all } w \in W_z \tag{22}$$

with W_z defined as follows:

$$W_z := \begin{cases} \{v|_{\omega_z} : v \in V, \|\varphi_z^{1/2} \varepsilon(v)\|_{L^2(\omega_z)} < \infty, \text{ and } v|_{\Gamma_D} = 0\} & \text{if } z \in \Gamma_D \\ \left\{v|_{\omega_z} : v \in V, \|\varphi_z^{1/2} \varepsilon(v)\|_{L^2(\omega_z)} < \infty, \text{ and } \int_{\omega_z} v \, dx = 0\right\} & \text{if } z \in \mathscr{H} \end{cases}$$

Let $\mathbb{R}^{n \times n}_{\mathrm{skew}}$ denote the set of skew symmetric matrices, the gradients of RBMs.

Theorem 4.2 (Generalized weighted Korn's inequality)
Given a Lipschitz domain $\Omega \subset \mathbb{R}^n$ and a positive weight function $\varphi \in C^0(\bar{\Omega})$ with $\varphi(x) > 0$ for all $x \in \Omega$, define

$$\hat{\Omega} := \{(x, x_{n+1}) \in \mathbb{R}^{n+1} : x \in \Omega, 0 < x_{n+1} < \varphi(x)\}$$

and assume that $\hat{\Omega}$ is also a Lipschitz domain in $\mathbb{R}^{n+1}$. Then there exists a constant C_{WKorn} such that

$$\min_{S \in \mathbb{R}^{n \times n}_{\mathrm{skew}}} \|\varphi^{1/2}(Dv - S)\|_{L^2(\Omega)} \leqslant C_{\mathrm{WKorn}} \|\varphi^{1/2} \varepsilon(v)\|_{L^2(\Omega)} \quad \text{for all } v \in V \tag{23}$$

Remark 4.3
A scaling argument reveals that C_{WKorn} depends on the shape of Ω and φ only but not on the size of Ω.

Proof
Given $v \in V$, define the function $\hat{v} \in H^1(\hat{\Omega}; \mathbb{R}^{n+1})$ by setting

$$\hat{v}(x, x_{n+1}) := (v(x), 0)$$

On $\hat{\Omega}$ there holds a Korn's inequality with a constant C_{GKorn} for $\hat{v}$. Thus, there exists a skew symmetric matrix $\hat{S} \in \mathbb{R}^{(n+1) \times (n+1)}_{\mathrm{skew}}$, such that

$$\|D\hat{v} - \hat{S}\|_{L^2(\hat{\Omega})} \leqslant C_{\mathrm{GKorn}} \|\hat{\varepsilon}(\hat{v})\|_{L^2(\hat{\Omega})} \tag{24}$$

Since $\hat{v}$ is independent of x_{n+1} and vanishes in the last component, the last row and the last column of the matrices $D\hat{u}$ and $\varepsilon(\hat{u})$ only vanish

$$D\hat{u} = \begin{pmatrix} & & & 0 \\ & Du & & \vdots \\ & & & 0 \\ 0 & \dots & 0 & 0 \end{pmatrix} \quad \text{and} \quad \hat{\varepsilon}(\hat{u}) = \begin{pmatrix} & & & 0 \\ & \varepsilon(u) & & \vdots \\ & & & 0 \\ 0 & \dots & 0 & 0 \end{pmatrix}$$

Table I. Numerical approximations of the eigenvalue problem (25) with the p-version of the FEM on four different meshes (not-displayed) on the reference triangle T_{ref} to illustrate the conjectured upper bound 5.

	Mesh 1		Mesh 2		Mesh 3		Mesh 4		
p	DOF	C_{ref}	DOF	C_{ref}	DOF	C_{ref}	DOF	C_{ref}	Δ^2
1	3	1.0000	6	1.7164	15	2.3232	45	3.2165	0.4310
2	6	2.2360	15	3.2967	45	3.9287	153	4.3574	5.2621
3	10	3.2124	28	3.8993	91	4.3254	325	4.5420	4.7660
4	15	3.5801	45	4.2000	153	4.4766	561	4.6089	4.7302
5	21	3.7573	66	4.3310	231	4.5459	861	4.6405	4.7149
6	28	3.9076	91	4.3939	325	4.5798	1225	4.6564	4.7103
7	36	3.9992	120	4.4330	435	4.5986	1653	4.6658	4.7118
8	45	4.0707	153	4.4601	561	4.6109	2145	4.6723	4.7145
9	55	4.1280	190	4.4809	703	4.6201	2701	4.6774	4.7176
10	66	4.1740	231	4.4977	861	4.6275	3321	4.6817	4.7204
11	78	4.2124	276	4.5118	1035	4.6338	4005	4.6853	4.7230
12	91	4.2446	325	4.5239	1225	4.6392	4753	4.6885	4.7252
13	105	4.2724	378	4.5344	1431	4.6440	5565	4.6913	4.7272
Δ^2		4.4440		4.6031		4.6786		4.7141	

Let the matrix $S \in \mathbb{R}_{\text{skew}}^{n \times n}$ be the leading upper submatrix of $\hat{S}$. Then

$$\int_{\hat{\Omega}} |D\hat{u} - \hat{S}|^2 \, \mathrm{d}\hat{x} = \int_{\Omega} \varphi(x) |Du - S|^2 \, \mathrm{d}x$$

and similar expression holds for $\|\hat{\varepsilon}(\hat{v})\|_{L^2(\hat{\Omega})}$. Then (24) reads

$$\int_{\Omega} \varphi(x) |Du - S|^2 \, \mathrm{d}\hat{x} \leqslant C_{\text{GKorn}}^2 \int_{\Omega} \varphi(x) |\varepsilon(u)|^2 \, \mathrm{d}x \qquad \square$$

4.4. Numerical computations of C_{Korn}

This subsection illustrates (23) numerically. By noticing $\varepsilon(g) = 0$ for $g \in \text{RBM}$, we reformulate (23) as follows: seek C_{ref} with

$$C_{\text{ref}}^2 = \max_{f \in H^2(T_{\text{ref}})^2/\text{RBM}} \min_{g \in \text{RBM}} \frac{\int_{T_{\text{ref}}} \varphi_{\text{ref}} |D(f - g)|^2 \, \mathrm{d}x}{\int_{T_{\text{ref}}} \varphi_{\text{ref}} |\varepsilon(f)|^2 \, \mathrm{d}x} \qquad (25)$$

Therein, $T_{\text{ref}} = \text{conv}\{(0, 0), (0, 1), (1, 0)\}$ denotes the reference triangle and φ_{ref} equals $\varphi_{\text{ref}}(x, y) = 1 - x - y$ for $(x, y) \in T_{\text{ref}}$.

This problem can be transformed into a generalized eigenvalue problem which is solved by FEMs with polynomial degree $p \geqslant 1$ on a series of fixed meshes graded towards the origin.

Table I displays numerical approximations for $p = 1, 2, \ldots, 13$ and the Aitken Δ^2 extrapolation values. Theorem 4.2 guarantees that $C_{\text{ref}} < \infty$ is a fixed constant.

4.5. Mesh-independence of C_{WKorn}

The previous two subsections illustrate that $C_{\text{WKorn}} < \infty$ depends in a mild way on φ_z. This subsection analyses that C_{WKorn} is bounded by C_{ref} and mesh parameters such as the minimal angle in the triangulation. The technique is to glue the estimates for individual elements together.

Lemma 4.4
Let T be a triangle of the triangulation $\mathcal{T}$ and let φ_z be the nodal basis function of some node $z \in T$. For all $f \in H^1(T; \mathbb{R}^d)$ there exists some RBM $g \in \mathrm{RBM}(T)$ with

$$\|\varphi_z^{1/2} D(f-g)\|_{L^2(T)} \leqslant C_T \|\varphi_z^{1/2} \varepsilon(f)\|_{L^2(T)} \tag{26}$$

The constant C_T depends on the shape of T but not on its size.

Proof
This follows from a transformation argument from (26) and $C_{\mathrm{ref}} < \infty$ with Theorem 4.2. The details are omitted. $\qquad\square$

Theorem 4.5
Given any $f \in H^1(\Omega)^2$, there exists some $g \in \mathrm{RBM}(\Omega)$ such that

$$\|\varphi_z^{1/2} D(f-g)\|_{L^2(\Omega)} \leqslant C \|\varphi_z^{1/2} \varepsilon(f)\|_{L^2(\Omega)} \tag{27}$$

The constant C is independent of f and g and solely depends on the shape of the elements but not on their size.

Proof
Let $\omega := \{x \in \Omega : \varphi_z(x) > \frac{1}{2}\} \subset \Omega$ and given $f \in H^1(\Omega; \mathbb{R}^d)$ employ Korn's inequality on ω (which has the same shape as ω_z) to find some $g \in \mathrm{RBM}(\Omega)$ such that

$$\|D(f-g)\|_{L^2(\omega)} \leqslant C_1 \|\varepsilon(f)\|_{L^2(\omega)} \tag{28}$$

For all $T \in \mathcal{T}$, Lemma 4.4 yields

$$\|\varphi_z^{1/2} D(f-g_T)\|_{L^2(T)} \leqslant C_2 \|\varphi_z^{1/2} \varepsilon(f)\|_{L^2(T)}$$

for some $g_T \in \mathrm{RBM}(T)$. Let $g_{\mathcal{T}} \in L^\infty(\Omega)$ be piecewise g_T, i.e.

$$g_{\mathcal{T}}|_T := g_T \quad \text{for all } T \in \mathcal{T}$$

and let $D_{\mathcal{T}}$ denote the piecewise gradient. Then the last estimate reads

$$\|\varphi_z^{1/2} D_{\mathcal{T}}(f-g_{\mathcal{T}})\|_{L^2(\Omega)} \leqslant C_2 \|\varphi_z^{1/2} \varepsilon(f)\|_{L^2(\Omega)} \tag{29}$$

A triangular inequality and (29) lead to

$$\|\varphi_z^{1/2} D(f-g)\|_{L^2(\Omega)} \leqslant \|\varphi_z^{1/2} D_{\mathcal{T}}(f-g_{\mathcal{T}})\|_{L^2(\Omega)} + \|\varphi_z^{1/2} D_{\mathcal{T}}(g-g_{\mathcal{T}})\|_{L^2(\Omega)}$$

$$\leqslant C_2 \|\varphi_z^{1/2} \varepsilon(f)\|_{L^2(\Omega)} + C_3 \|D_{\mathcal{T}}(g-g_{\mathcal{T}})\|_{L^2(\Omega)}$$

In the last step we used that $D_{\mathcal{T}}(g-g_{\mathcal{T}})$ is piecewise constant and employed

$$C_3^2 := \max_{T \in \mathcal{T}} \int_T \varphi_z(x) \, \mathrm{d}x / |T \cap \omega|$$

From (28)

$$\|D_{\mathscr{T}}(g - g_{\mathscr{T}})\|_{L^2(\omega)} \leqslant \|D_{\mathscr{T}}(g_{\mathscr{T}} - f)\|_{L^2(\omega)} + \|D(g - f)\|_{L^2(\omega)}$$

$$\leqslant \sqrt{2}\|\varphi_z^{1/2} D_{\mathscr{T}}(g_{\mathscr{T}} - f)\|_{L^2(\omega)} + C_1\|\varepsilon(f)\|_{L^2(\omega)}$$

$$\leqslant \sqrt{2}C_2\|\varphi_z^{1/2}\varepsilon(f)\|_{L^2(\Omega)} + C_1\sqrt{2}\|\varphi_z^{1/2}\varepsilon(f)\|_{L^2(\omega)}$$

$$= (C_1 + C_2)\sqrt{2}\|\varphi_z^{1/2}\varepsilon(f)\|_{L^2(\omega)}$$

Altogether, one proves the assertion with $C = C_2 + C_3\sqrt{2}(C_1 + C_2)$. $\qquad\square$

4.6. Efficiency of μ_{L}

This subsection aims at an analysis of the efficiency of μ_{L}.

Theorem 4.6 (Efficiency of μ_{L})
Assume u is the solution of the model problem and u_h a numerical approximation of u obtained by an appropriate FEM. Then there holds for every node z

$$A_z := \sup_{w \in W_z} \|\mathbb{C}^{1/2}\varepsilon(\varphi_z v)\|_{L^2(\varphi_z)} / \|\mathbb{C}^{1/2}\varphi_z^{1/2}\varepsilon(v)\|_{L^2(\omega_z)} < \infty \tag{30}$$

and

$$\mu_z \leqslant A_z\|\mathbb{C}^{1/2}\varepsilon(u - u_h)\|_{L^2(\omega_z)} \tag{31}$$

With $C_A := \max_{z \in \mathscr{N}} A_z$ there holds a global efficiency of μ_{L} in the sense of

$$\mu_{\mathrm{L}} \leqslant \sqrt{3}C_A\|\mathbb{C}^{1/2}\varepsilon(u - u_h)\|_{L^2(\Omega)} \tag{32}$$

Proof
An integration by parts and Cauchy inequalities with (30) yield

$$\mathrm{Res}_z(v) = \int_{\omega_z} \varphi_z(f + \mathrm{div}_{\mathscr{T}}\sigma_h) \cdot v \, \mathrm{d}x - \int_{\cup \mathscr{E} \cap \omega_z} \varphi_z[\sigma_h] \cdot v \, \mathrm{d}s$$

$$= \int_{\omega_z} \mathbb{C}\varepsilon(u - u_h) : \varepsilon(\varphi_z v) \, \mathrm{d}x$$

$$\leqslant \|\mathbb{C}^{1/2}\varepsilon(u - u_h)\|_{L^2(\omega_z)} \|\mathbb{C}^{1/2}\varepsilon(\varphi_z v)\|_{L^2(\omega_z)}$$

$$\leqslant \|\mathbb{C}^{1/2}\varepsilon(u - u_h)\|_{L^2(\omega_z)} A_z\|\mathbb{C}^{1/2}\varphi_z^{1/2}\varepsilon(v)\|_{L^2(\omega_z)}$$

A division by $\|\mathbb{C}^{1/2}\varphi_z^{1/2}\varepsilon(v)\|_{L^2(\omega_z)}$ yields (31). Equation (32) follows as (18) in the proof of Theorem 3.3. It remains to prove (30) with the same techniques as in the proof of (16). We have

$$\|\mathbb{C}^{1/2}\varepsilon(\varphi_z v)\|_{L^2(\omega_z)} = \|\mathbb{C}^{1/2}(\varphi_z\varepsilon(v) + (v \otimes D\varphi_z)^{(s)})\|_{L^2(\omega_z)}$$

$$\leqslant \|\mathbb{C}^{1/2}\varphi_z\varepsilon(v)\|_{L^2(\omega_z)} + \|\mathbb{C}^{1/2}(v \otimes D\varphi_z)^{(s)}\|_{L^2(\omega_z)}$$

$$\leqslant \|\mathbb{C}^{1/2}\varphi_z\varepsilon(v)\|_{L^2(\omega_z)} + \|\mathbb{C}^{1/2}D\varphi_z\|_{L^\infty(\omega_z)}\|v\|_{L^2(\omega_z)}$$

where $(v \otimes D\varphi_z)^{(s)}$ denotes the symmetric part of $v \otimes D\varphi_z$. Theorem 3.2 followed by (22) yields

$$\|v\|_{L^2(\omega_z)} \leqslant C_{\mathrm{PF}} h_z \|\varphi_z^{1/2} Dv\|_{L^2(\omega_z)}$$

$$\leqslant C_{\mathrm{PF}} h_z C_{\mathrm{WKorn}} \|\varphi_z^{1/2} \varepsilon(v)\|_{L^2(\omega_z)}$$

$$\leqslant \frac{C_{\mathrm{PF}} h_z C_{\mathrm{WKorn}}}{\sqrt{2\mu}} \|\mathbb{C}^{1/2} \varphi_z^{1/2} \varepsilon(v)\|_{L^2(\omega_z)}$$

Altogether one deduces

$$A_z \leqslant 1 + \sqrt{2(1 + \lambda/\mu)} \|D\varphi_z\|_{L^\infty(\omega_z)} C_{\mathrm{PF}} h_z C_{\mathrm{WKorn}} \qquad \Box$$

5. NUMERICAL REALIZATION

Since the localized estimators are implicit, i.e. they require the exact solution of local problems, we need to study numerical approximations $\tilde{\eta}_{\mathrm{L}}$ and $\tilde{\mu}_{\mathrm{L}}$ to those estimates η_{L} and μ_{L}, respectively.

5.1. Solvability of local problems to compute η_z and μ_z

The computation of η_z and μ_z requires the numerical solution of a local problem. Recall V_z and W_z from Sections 3.3 and 4.3.

Problem $(P_z^{(1)})$
Seek $w \in V_z$, such that

$$a_z(w, v) := \int_{\omega_z} \varphi_z(x) Dw(x) : Dv(x)\, \mathrm{d}x = \mathrm{Res}_z(v) \quad \text{for all } v \in V_z \qquad (33)$$

Problem $(P_z^{(2)})$
Seek $w \in W_z$, such that

$$a_z(w, v) := \int_{\omega_z} \varphi_z(x) \varepsilon(w(x)) : \mathbb{C}\varepsilon(v(x))\, \mathrm{d}x = \mathrm{Res}_z(v) \quad \text{for all } v \in W_z \qquad (34)$$

Define $\|\cdot\|_z := a_z(\cdot, \cdot)^{1/2}$ and note that $\eta_z = \|w\|_z$ in (20) for Problem $(P_z^{(1)})$. To see that $\eta_z = \|w\|_z$ for Problem $(P_z^{(2)})$ as well, we first need to study the kernel Z_z of a_z. It is relatively straightforward to check $\{v \in H^1_{\mathrm{loc}}(\omega_z) : a_z(v, \cdot) = 0 \in W_z^*\} = \mathrm{RBM}$.

Hence, it is necessary for (34) is that Res_z vanishes for RBM, i.e.

$$\mathrm{RBM} \subset \ker \mathrm{Res}_z \quad \text{for each } z \in \mathcal{K} \qquad (35)$$

Sufficient for (35) is that $\varphi_z v$ is a finite element function for all $v \in \mathrm{RBM}$. ($\mathrm{Res}_z(v) = \int_\Omega \mathbb{C}\varepsilon(u - u_h) : \varepsilon(\varphi_z v)\, \mathrm{d}x$ vanishes as a consequence of the Galerkin equations.) The condition

$$(\mathrm{RBM})\varphi_z \subseteq V_h \quad \text{for each } z \in \mathcal{K} \qquad (36)$$

is sufficient for (35) and in fact sufficient for the unique solvability of $(P_z^{(2)})$.

Note that (36) is satisfied for P_2 and, by design, for the new $P_1 + $ RBM FEM. The P_1 FEM is excluded and, in fact, (35) generally fails to hold.

Theorem 5.1 (Existence and uniqueness for $(P_z^{(2)})$)
Assume that (RBM)$\varphi_z \subseteq V_h$ for $z \in \mathscr{K}$. Then Problem $(P_z^{(2)})$ has a unique solution $w \in W_z$ and

$$\mu_z = \|\varphi(z)^{1/2} \mathbb{C}^{1/2} \varepsilon(w)\|_{L^2(\omega_z)} = \|w\|_z \tag{37}$$

Proof
The symmetric bilinear form a_z is W_z-elliptic because

$$a_z(w, w) := \int_{\omega_z} \varphi_z(x) \mathbb{C}\varepsilon(w(x)) : \varepsilon(w(x)) \, dx \geqslant 2\mu \|\varphi_z^{1/2} \varepsilon(w)\|^2_{L^2(\omega_z)}$$

followed by the weighted Friedrichs inequality and the weighted Korn inequality. Thus, the Lax–Milgram lemma can be applied which leads to the unique existence of w. With the Cauchy–Schwarz inequality with respect to the scalar product $a_z(\cdot, \cdot)$, we have for all $v \in W_z$ with $\|v\|_z > 0$

$$R_z(v)^2 / a_z(v, v) = a_z(w, v)^2 / a_z(v, v) \leqslant (a_z(w, w) a_z(v, v)) / a_z(v, v) = a_z(w, w)$$

Hence, $\mu_z := \sup_{v \in W_z} R_z(v)^2 / a_z(v, v) = a_z(w, w) = \|\varphi_z^{1/2} \mathbb{C}^{1/2} \varepsilon(w)\|^2_{L^2(\omega_z)}$. $\qquad \square$

So far, the computation of the error estimators was performed solving local problems exactly. In practice, one computes approximative solutions using a FEM of higher order (in our example, we used P_4 elements). This yields approximations $\tilde{\eta}_L$ and $\tilde{\mu}_L$ to η_L and μ_L. In the following, we will examine the efficiency and reliability of these estimators.

Theorem 5.2 (Efficiency of $\tilde{\eta}_L$ and $\tilde{\mu}_L$)
As η_L and μ_L are efficient according to Lemma 3.3 and Lemma 4.6, $\tilde{\eta}_L$ and $\tilde{\mu}_L$ are also efficient.

Proof
The estimators η_L and μ_L are computed by solving local problems $(P_z^{(1)})$ and $(P_z^{(2)})$ on the space W_z. Since $\tilde{\eta}_L$ and $\tilde{\mu}_L$ are each solved on a subspace $\tilde{W}_z \subset W_z$

$$\tilde{\eta}_L \leqslant \eta_L \quad \text{and} \quad \tilde{\mu}_L \leqslant \mu_L \qquad\qquad \square$$

5.2. Reliability of $\tilde{\eta}_L \leqslant \eta_L$

Throughout this section, we restrict to the P_1 FEM where u_h is piecewise affine and $\sigma_h := \mathbb{C}\varepsilon(u_h)$ is piecewise constant. On each patch ω_z, Problem $(P_z^{(1)})$ is solved for a unique solution $w \in V_z$ and $\eta_z = \|w\|_z$, while $\tilde{\eta}_z := \|\tilde{w}\|_z$ for $\tilde{w}$ in $\tilde{W}_z$ for a fourth-order FES $\tilde{W}_z \subset W_z$.

Theorem 5.3 (Reliability of $\tilde{\eta}_L$)
η_z is bounded by

$$\eta_z = \|w_z\|_z \leqslant C \|\tilde{w}_z\|_z + \text{h.o.t.} = C\tilde{\eta}_z + \text{h.o.t.} \quad \text{for all } z \in \mathscr{N} \tag{38}$$

The remaining part of this subsection is devoted to the proof of Theorem 5.3 and the study of minimal conditions on W sufficient for (38).

Let $\mathcal{N}_z$ denote the set of nodes in $\overline{\omega}_z$ and let $\mathcal{E}_z$ be the set of all edges with z as one vertex. With the nodal basis function $\varphi_j(x)$, $j \in \mathcal{N}_z$, define

$$\Phi_z(x) := 18 \sum_{j \in \mathcal{N}_z, j \neq z} \varphi_j(x) - 6$$

Given any $E \in \mathcal{E}_z$, let the other vertex of E be z_E and denote the first adjoint triangle with T_1 and the second one, if it exists, with T_2, otherwise set $|T_2| := 0$. Then define

$$\Phi_E(x) := 6\varphi_{z_E} - \frac{|T_1| + |T_2|}{2|\omega_z|} \Phi_z$$

Straightforward calculations verify

$$\int_{\omega_z} \varphi_z \Phi_z \, \mathrm{d}x = |\omega_z|$$

$$\int_F \varphi_z \Phi_z \, \mathrm{d}s = 0 \quad \text{for all edges } F \in \mathcal{E}_z$$

$$\int_{\omega_z} \varphi_z \Phi_E \, \mathrm{d}x = 0$$

$$\int_F \varphi_z \Phi_E \, \mathrm{d}s = \begin{cases} |E| & \text{for } E = F \in \mathcal{E}_z \\ 0 & \text{for all edges } F \in \mathcal{E}_z \setminus \{E\} \end{cases}$$

Lemma 5.4
Define $f_z := 1/|\omega_z| \int_{\omega_z} f(x) \, \mathrm{d}x$ and denote the jth canonical unit vector with e_j. Then

$$R_z(\Phi_z e_j) = \int_{\omega_z} (f - f_z) \varphi_z \Phi_z e_j \, \mathrm{d}x + f_z \cdot e_j |\omega_z| \tag{39}$$

$$R_z(\Phi_E e_j) = \int_{\omega_z} (f - f_z) \varphi_z \Phi_E e_j \, \mathrm{d}x - ([\sigma_h]\nu_E) \cdot e_j |E| \tag{40}$$

Proof
Using the aforementioned identities and the fact that u_h is affine on each triangle

$$R_z(\Phi_z e_j) = (\mathrm{div}_{\mathcal{T}} \sigma(u_h), \varphi_z \Phi_z e_j)_{L^2(\Omega)} + (f, \varphi_z \Phi_z e_j)_{L^2(\Omega)} - \sum_{F \in \mathcal{E}_z} \int_F \varphi_z([\sigma_h]\nu_F) \cdot \Phi_z e_j \, \mathrm{d}s$$

In fact, $\mathrm{div}_{\mathcal{T}} \sigma(u_h)$ is zero and $[\sigma_h]\nu_F$ is constant along F and hence $\int_F \Phi_z \varphi_z [\sigma_h]\nu_F \cdot e_j \, \mathrm{d}s = 0$. Consequently,

$$R_z(\Phi_z e_j) = (f - f_z, \varphi_z \Phi_z e_j)_{L^2(\Omega)} + (f_z, \varphi_z \Phi_z e_j)_{L^2(\Omega)}$$

$$= (f - f_z, \varphi_z \Phi_z e_j)_{L^2(\Omega)} + f_z \cdot e_j |\omega_z|$$

The same arguments lead to

$$R_z(\Phi_E e_j) = (\mathrm{div}_{\mathscr{T}}\sigma(u_h), \varphi_z \Phi_E e_j)_{L^2(\Omega)} + (f, \varphi_z \Phi_E e_j)_{L^2(\Omega)} - \sum_{F \in \mathscr{E}_z} \int_F \varphi_z [\sigma_h] v_F \Phi_E e_j \, \mathrm{d}s$$

$$= (f - f_z, \varphi_z \Phi_E e_j)_{L^2(\Omega)} - ([\sigma_h] v_E) \cdot e_j |E| \qquad \square$$

Given any $u_z \in H^1_{\mathrm{loc}}(\omega_z; \mathbb{R}^d)/\mathbb{R}^d$ with $\|u_z\|_z = 1$ set

$$v_z := \frac{1}{|\omega_z|}\Phi_z \int_{\omega_z} \varphi_z u_z \, \mathrm{d}x + \sum_{E \in \mathscr{E}_z} \frac{1}{|E|}\Phi_E \int_E \varphi_z u_z \, \mathrm{d}s$$

Lemma 5.5
We have

$$R_z(u_z) = R_z(v_z) + \mathrm{h.o.t.}$$

Proof
Lemma 5.4 and the aforementioned properties of Φ_E and Φ_z lead to

$$R_z(u_z) = (\mathrm{div}_{\mathscr{T}}\sigma(u_h), \varphi_z u_z)_{L^2(\Omega)} + (f, \varphi_z u_z)_{L^2(\Omega)} - \sum_{E \in \mathscr{E}_z} \int_E \varphi_z ([\sigma_h] v_E) \cdot u_z \, \mathrm{d}s$$

$$= (f - f_z, \varphi_z u_z)_{L^2(\Omega)} + (f_z, \varphi_z u_z)_{L^2(\Omega)} - \sum_{E \in \mathscr{E}_z} [\sigma_h] v_E \cdot \int_E \varphi_z u_z \, \mathrm{d}s$$

$$= \frac{1}{|\omega_z|}\int_{\omega_z}(f - f_z)\varphi_z u_z \, \mathrm{d}x \int_{\omega_z} \varphi_z \Phi_z \, \mathrm{d}x$$

$$+ \left(\frac{1}{|\omega_z|}\mathrm{Res}_z(\Phi_z)\int_{\omega_z} \varphi_z u_z \, \mathrm{d}x - \frac{1}{|\omega_z|}\int_{\omega_z}(f - f_z)\varphi_z \Phi_z \, \mathrm{d}x \int_{\omega_z} \varphi_z u_z \, \mathrm{d}s\right)$$

$$+ \sum_{E \in \mathscr{E}_z}\left(\frac{1}{|E|}\mathrm{Res}_z(\Phi_E)\int_E \varphi_z u_z \, \mathrm{d}s - \frac{1}{|E|}\int_{\omega_z}(f - f_z)\varphi_z \Phi_E \, \mathrm{d}x \int_E \varphi_z u_z \, \mathrm{d}s\right)$$

Since

$$\mathrm{Res}_z(v_z) = \frac{1}{|\omega_z|}\mathrm{Res}_z(\Phi_z)\int_{\omega_z} \varphi_z u_z \, \mathrm{d}x + \sum_{E \in \mathscr{E}_z} \frac{1}{|E|}\mathrm{Res}_z(\Phi_E)\int_E \varphi_z u_z \, \mathrm{d}s$$

the above identity verifies

$$\mathrm{Res}_z(u_z) = \mathrm{Res}_z(v_z) + \mathrm{h.o.t.}$$

with the higher-order (i.e. second-order) term

$$\mathrm{h.o.t.} := \frac{1}{|\omega_z|}\int_{\omega_z}(f - f_z)\varphi_z u_z \, \mathrm{d}x \int_{\omega_z} \varphi_z \Phi_z \, \mathrm{d}x - \frac{1}{|\omega_z|}\int_{\omega_z}(f - f_z)\varphi_z \Phi_z \, \mathrm{d}x \int_{\omega_z} \varphi_z u_z \, \mathrm{d}x$$

$$- \sum_{E \in \mathscr{E}_z} \frac{1}{|E|}\int_{\omega_z}(f - f_z)\varphi_z \Phi_E \, \mathrm{d}x \int_E \varphi_z u_z \, \mathrm{d}s \qquad \square$$

Lemma 5.6
Under the assumption of a minimum angle condition in the patch ω_z, we have $\|v_z\|_z \leqslant C$ with a real constant C.

Proof
Straightforward calculations reveal $\|D\Phi_z\|_{L^2(\omega_z)} + \|D\Phi_E\|_{L^2(\omega_z)} \lesssim h_z^{-1}|\omega_z|^{1/2} \lesssim 1$, $h_E \approx h_T$ etc., and the assertion reads $\|v_z\|_z \lesssim 1$. Using Cauchy's inequality, Young's inequality, Friedrichs' inequality and the trace inequality, one deduces (where T_E is some neighbour element of E)

$$\|v_z\|_z \lesssim \|D\Phi_z\|_{L^2(\omega_z)} \left| \frac{1}{|\omega_z|} \int_{\omega_z} \varphi_z u_z \, \mathrm{d}x \right| + \sum_{E \in \mathscr{E}_z} \|D\Phi_E\|_{L^2(\omega_z)} \left| \frac{1}{|E|} \int_E \varphi_z u_z \, \mathrm{d}s \right|$$

$$\lesssim h_z^{-1}|\omega_z|^{-1/2} \int_{\omega_z} |\varphi_z||u_z| \, \mathrm{d}x + h_z^{-1}|\omega_z|^{1/2} \sum_{E \in \mathscr{E}_z} h_E^{-1} \int_E |\varphi_z||u_z| \, \mathrm{d}s \|\varphi_z^{1/2} u_z\|_{L^2(E)}$$

$$\lesssim \|\varphi_z^{1/2} Du_z\|_{L^2(\omega_z)} + \sum_{E \in \mathscr{E}_z} (h_E^{-1}\|\varphi_z^{1/2} u_z\|_{L^2(T_E)} + \|D(\varphi_z^{1/2} u_z)\|_{L^2(T_E)})$$

$$\lesssim \|Du_z\|_{L^2(\omega_z)} \lesssim 1 \qquad \qquad \qquad \square$$

Proof of Theorem 5.3
This follows from Lemmas 5.5 and 5.6:

$$\|w_z\|_z = \|R_z\|_{W_z^*} = \sup_{\|u_z\|_z \neq 0} \frac{|R_z(u_z)|}{\|u_z\|_z} \leqslant \sup_{\|u_z\|_z \neq 0} \frac{|R_z(v_z) + \text{h.o.t.}|}{\|u_z\|_z}$$

$$\leqslant \sup_{\|u_z\|_z \neq 0} \frac{\|R_z\|_{\tilde{W}_z^*}\|v_z\|_z}{\|u_z\|_z} + \text{h.o.t.} \leqslant C\|\tilde{w}_z\|_z + \text{h.o.t.} \qquad \square$$

It is stressed that the theorem requires only that Φ_E belongs to the FES employed to solve the local problems.

5.3. Reliability of $\tilde{\eta}_L$, $\tilde{\mu}_L$ for other situations

The arguments of Section 5.2 essentially apply for the other FE schemes to compute u_h as well as on the spaces $\tilde{V}_z$ and $\tilde{W}_z$ which determine η_L and μ_L. However, the design of Φ_z and Φ_E may be more involved. In order to cancel the possibly non-constant terms $\mathrm{div}\,\sigma_h|_T$ and $[\sigma_h] \cdot \nu_E$ on E one requires Φ_z and Φ_E to have higher-order cancellation properties, e.g. $\int_T \varphi_z \Phi_z q \, \mathrm{d}x = \int_T \varphi_z \Phi_E q \, \mathrm{d}x = 0$ for all $q \in P_1(T)$ and $\int_E \varphi_z \Phi_z r \, \mathrm{d}x = 0$ for all $r \in P_1(E)$. By adding proper element-bubble functions and proper edge-bubble functions, this can indeed be achieved. At the end, it is required that Φ_z and all the employed Φ_E belong to $\tilde{V}_z$ and $\tilde{W}_z$. Fourth-order FEs are sufficient for that and, eventually, guarantee reliability up date oscillations. We omit further details because of their purely technical character.

6. NUMERICAL EXPERIMENTS FOR RELIABILITY AND EFFICIENCY

The energy error and error estimators are computed for P_1, $P_1 + \text{RBM}$, and P_2 finite elements for four examples on an L-shaped domain $\Omega = (-1, 0) \times (-1, 1) \cup [0, 1) \times (0, 1)$, for the Cock's membrane problem and the slit domain $\Omega = (-1, +1)^p|_{[0,1) \times \{0\}}$. The implementations follows [9, 12, 13] in MATLAB with element-oriented adaptive algorithms from [9].

6.1. L-shape example

The L-shaped domain Ω without Neumann conditions (i.e. $\partial\Omega = \Gamma_D$) leads to $C_{\text{Korn}} = \sqrt{2}$ and $C_{\text{Kornelast}} = C_{\text{Korn}}/\sqrt{2\mu} = 0.0050990195$ has been confirmed by our numerical experiments for Young's modul $E = 100\,000$ and Poisson ration $\mu = 0.3$. The pure Dirichlet problem (1)–(3) is specified by $f \equiv 0$ and u_D given by the exact solution which reads in polar co-ordinates (r, φ)

$$u_r(r, \varphi) = \frac{r^\alpha}{2\mu}(-(1 + \alpha)\cos((1 + \alpha)\varphi) + (c_2 - (1 + \alpha))c_1\cos((\alpha - 1)\varphi))$$

$$u_\varphi(r, \varphi) = \frac{r^\alpha}{2\mu}((1 + \alpha)\sin((1 + \alpha)\varphi) + (c_2 + \alpha - 1)c_1\sin((\alpha - 1)\varphi))$$
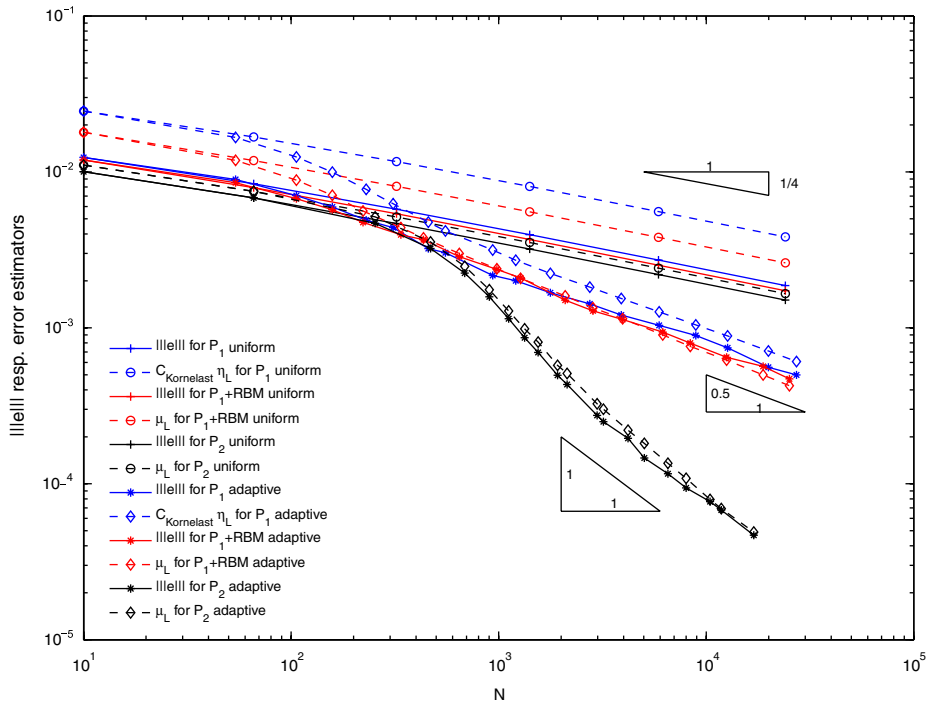

Figure 1. Convergence history for energy error $\|\|e\|\|$ and estimators $C_{\text{Kornelast}}\tilde{\eta}_L$ and $\tilde{\mu}_L$ as functions of the number of degrees of freedom N for P_1, $P_1 + \text{RBM}$, and P_2 FEM on uniform and adapted meshes in the L shape example of Section 6.1.

for the exponent $\alpha = 0.544483737$ which solves $\alpha \sin(2\omega) + \sin(2\omega\alpha) = 0$ for $\omega = 3\pi/4$ and for $c_1 = 2(\lambda+2\mu)/(\lambda+\mu)$. We refer to [13] for meshes, algorithms and further details in this benchmark and focus on the compressed output displayed in Figure 1. The convergence rates ($\equiv$ twice the negative slope) in this double logarithmic scales of all the plots of the convergence history confirm the theoretical expectations based on the singularity r^{α} of the exact solution. For uniform mesh refinements the three FE schemes support the convergence rate α (i.e. the slope $-\alpha/2$) while the adaptive meshes display the optimal convergence rate 1 for P_1 and $P_1 + \text{RBM}$ and 2 for P_2 FEM. The energy error $\|\|e\|\|$ and its numerical upper bound $C_{\text{Kornelast}}\tilde{\eta}_L$ are relatively close for the $P_1 + \text{RBM}$ and the P_2 FEM. A comparison with $\tilde{\mu}_L$ suggests $\|\|e\|\| \leqslant \tilde{\mu}_L \leqslant C_{\text{Kornelast}}\tilde{\eta}_L$ with a good agreement of $\|\|e\|\|$ and $\tilde{\mu}_L$.

6.2. Cook's membrane example

The data of the Cook's membrane benchmark example can be found in the literature [12, 13]; f, E, v are as in Section 6.1. Numerical experiments supported $C_{\text{Korn}} = 5.2974$ and $C_{\text{Kornelast}} = 0.116394014$ which is 21% smaller than $C_{\text{Korn}}/\sqrt{2\mu}$. The convergence history of Figure 2 is computed from $\|\|e\|\|^2 = \|\|u\|\|^2 - \|\|u_h\|\|^2$ with the value $\|\|u\|\| = 1.34751271200664$ from careful extrapolated simulations. In contrast to the good accuracy of the estimators $\tilde{\mu}_L$ and $\tilde{\eta}_L$ in the example of Section 6.1, the estimation of this subsection, although supporting $\|\|e\|\| \leqslant \tilde{\mu}_L \leqslant C_{\text{Kornelast}}\tilde{\eta}_L$, is
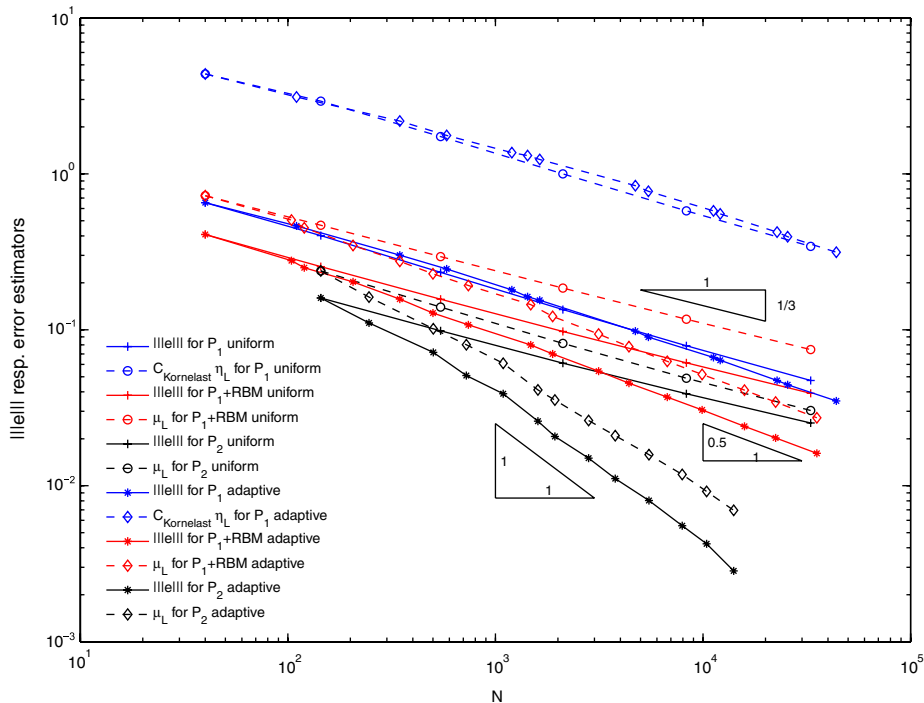

Figure 2. Convergence history for the energy error $\|\|e\|\|$ and estimators $C_{\text{Kornelast}}\tilde{\eta}_L$ and $\tilde{\mu}_L$ as functions of the number of degrees of freedom N for P_1, $P_1 + \text{RBM}$, and P_2 FEM on uniform and adapted meshes in the Cook's membrane problem in Section 6.2.
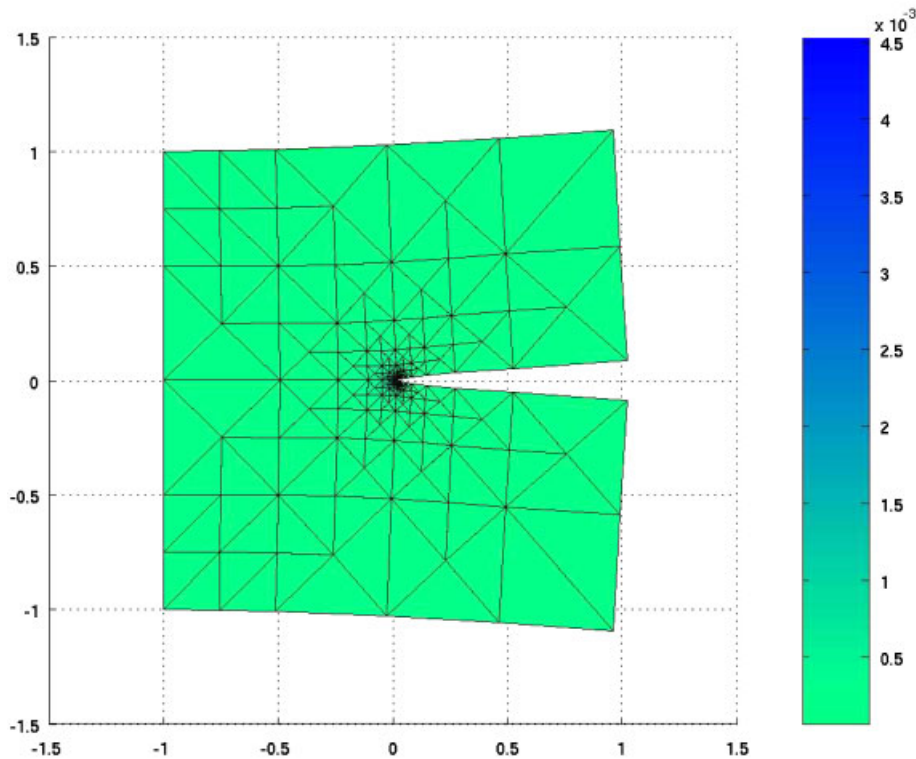
Figure 3. Deformed adapted mesh for $P_{1+\text{RB}}$ elements of the slit domain of Section 6.3 with 360 degrees of freedom and a displacement magnification by the factor 1000.

less accurate with overestimation of the magnitude of [7] for the Laplace problem. The estimation is better for adapted meshes and the various experimental convergence rates seem in agreement with expectations from the literature.

6.3. Slit domain example

The slit domain $\Omega = (-1, +1)^2 \backslash [0, 1) \times \{0\}$ of an elastic material with f, E, v from the previous examples is displayed in a deformed configuration in Figure 3. The Dirichlet boundary is on the left side with $u_D \equiv 0$ on $\Gamma_D := \{-1\} \times (-1, +1)$ while the surface lead vanishes except for $\{x \in \partial\Omega : x = \pm 1\}$ where $g(x) = (0, \pm 1)$. Numerical simulations support $C_{\text{Korn}} = 5.3458$ and $C_{\text{Kornelast}} = 0.01927466033063$ which overestimates $C_{\text{Korn}}/\sqrt{2\mu}$ by a factor 1.19. (This illustrates numerical difficulties and $\|u\| = 0.0119655862938$.) The convergence history of Figure 4 allows similar conclusions as before, but $\tilde{\mu}_L$ is very close to $\|e\|$ ($\tilde{\eta}_L$ is scaled by an overestimated factor C_{Korn}).

6.4. Locking

One important effect in the numerical computation of solutions in linear elasticity is locking: as Poisson's ratio v tends to 0.5 and the solution is obtained with Lagrange elements, the solution
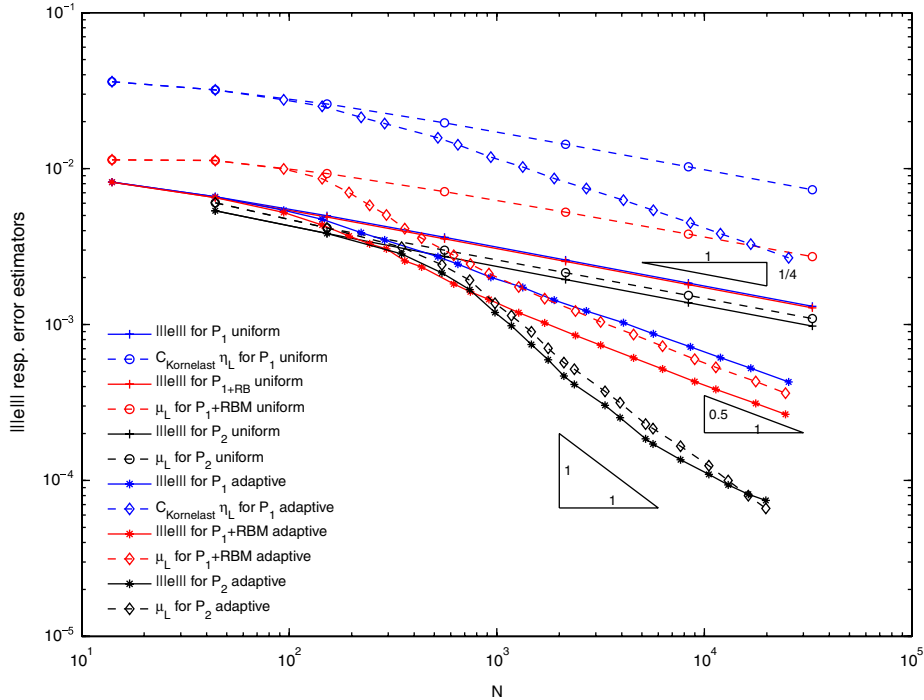
Figure 4. Convergence history for the energy error $\||e\||$ and estimators $C_{\text{Kornelast}}\tilde{\eta}_L$ and $\tilde{\mu}_L$ as functions of the number of degrees of freedom N for P_1, $P_1 + \text{RBM}$, and P_2 FEM on uniform and adapted meshes in slit domain from Section 6.3.

degenerates. Figure 5 shows the energy error for the three types of elements with adaptive refinement for the values $v = \{0.4, 0.45, 0.49, 0.499, 0.4999\}$. An examination of the new $P_1 + \text{RBM}$ FEM elements shows that they also have this locking property while the adaptive P_2 FEM compensate for this effect best.

Similar remarks apply to the uniform mesh refinements (not displayed). For large meshes of degrees of freedom (say $N \geqslant 30\,000$) the convergence rate is much improved in Figure 5; the reasons for this remain unclear, although adaptive FE schemes are observed to have a positive effect for the locking phenomenon [13].

7. DISCUSSION

The localized P_1-error estimator is a reliable error estimator, but requires the global Korn's constant. This difficulty is circumvented and localized by using our proposed $P_1 + \text{RBM}$ FEM. The numerical experiments show that the solution itself is not much better than the solution with P_1 FEM. The localized error estimator μ_L, however, estimates the energy error very accurately. The use of P_2 FEM shows the best results, μ_L is again a good reliable error estimator.

A comparison of the computation times of the three methods to compute a solution with a given error tolerance shows that the P_2-method needs the least time. At first glance this appears strange
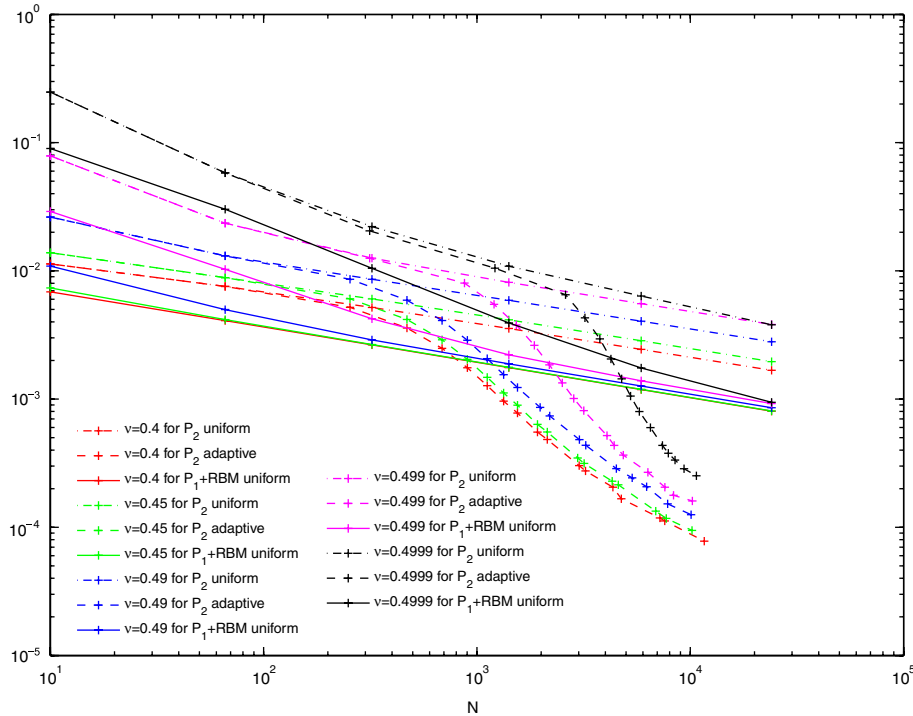
Figure 5. Convergence history for the energy error $\||e\||$ as a function of the number of degrees of freedom N for P_1, P_1+RBM, and P_2 FEM on uniform and adapted meshes in locking example on L-shaped domain in Section 6.4 for adaptive mesh-refining for various Poisson rations v=0.4, 0.45, 0.49, 0.499 and 0.4999.

but can be explained like this: if one looks at the computation time of one iteration in all the three cases, it can be seen that between 80 and 90% of the time is consumed by the computation of the error estimator. Considering one triangle, it bears 9 degrees of freedom in the $P_1 +$ RBM FEM case and requires the solution of three local problems for the error estimator, while in the P_2 case a triangle has 12 degrees of freedom but also generates only three local problems. This means that a certain number of degrees of freedom (and thus a certain quality of the solution) requires a higher number of elements in the $P_1 +$ RBM FEM, etc. and thus a lot more local problems to be solved—and this results in a much higher computation time. One possible conclusion from the numerical experiments is the recommendation of the adaptive P_2 FEM combined with the localized error estimator proposed in this paper.

REFERENCES

1. Ainsworth M, Oden JT. *A Posteriori Error Estimation in Finite Element Analysis*. Wiley-Interscience: New York, 2000; xx + 240.
2. Babuška I, Strouboulis T. *The Finite Element Method and its Reliability*. The Clarendon Press, Oxford University Press: Oxford, 2001; xii + 802.
3. Eriksson K, Estep D, Hansbo P, Johnson C. *Introduction to Adaptive Methods for Differential Equations*. Acta Numerica. Cambridge University Press: Cambridge, 1995; 105–158.
4. Eriksson K, Estep D, Hansbo P, Johnson C. *Computational Differential Equations*. Cambridge University Press: Cambridge, 1996; xvi + 538.
5. Verfürth R. A review of a posteriori error estimation techniques for elasticity problems. *Computer Methods in Applied Mechanics and Engineering* 1999; **176**:419–440.
6. Braess D. *Finite Elements—Theory*, *Fast Solvers and Applications in Solid Mechanics*. Cambridge University Press: Cambridge, 2001.
7. Bartels S, Carstensen C, Klose R. An experimental survey of a posteriori Courant finite element error control for the Poisson equation. *Advances in Computational Mathematics* 2001; **15**:79–106.
8. Klose R. A posteriori finite elemente analysis zur adaptiven Ortsdiskretisierung in der Elastoviskoplastizität. *Ph.D. Thesis*, Christian-Albrechts-Universität zu Kiel, Kiel, 2003.
9. Carstensen C, Funken SA. Fully reliable localized error control in the FEM. *SIAM Journal on Scientific Computing* 2000; **21**:1465–1484.
10. Morin P, Nochetto R, Siebert K. Local problems on stars: a posteriori error estimators, convergence, and performance. *Mathematics of Computation* 2003; **72**:1067–1097.
11. Parés N, Díez P, Huerta A. Subdomain-based flux-free a posteriori error estimators. *Computer Methods in Applied Mechanics and Engineering* 2006; **195**:297–323.
12. Alberty J, Carstensen C, Funken SA, Klose R. Matlab implementation of the finite element method in elasticity. *Computing* 2002; **69**(3):239–263.
13. Carstensen C, Funken SA. Averaging technique for FE a posteriori error control in elasticity. I. Conforming FEM. *Computer Methods in Applied Mechanics and Engineering* 2001; **190**(18–19):2483–2498. Averaging technique for FE-A posteriori error control in elasticity. II. λ-independent estimates. *Computer Methods in Applied Mechanics and Engineering* 2001; **190**(35–36):4663–4675. Averaging technique for a posteriori error control in elasticity. III. Locking-free nonconforming FEM. *Computer Methods in Applied Mechanics and Engineering* 2001; **191**(8–10):861–877.